ECEE2026
18th European Conference on Earthquake Engineering

A COMPREHENSIVE GLOBAL VULNERABILITY MODEL FOR IMPROVED EARTHQUAKE LOSS MODELLING

Al Mouayed Bellah Nafeh[1], Karim Aljawhari[1,2], Vitor Silva[1,3]

1- Global Earthquake Model (GEM) Foundation, Italy

2- Department of Civil, Environmental, and Geomatic Engineering, University College London (UCL), London, UK

3- Department of Civil Engineering, University of Aveiro, Aveiro, Portugal

mouayed.nafeh@globalquakemodel.org

Abstract

Vulnerability functions are essential for earthquake risk assessments; however, many existing models rely on simplified numerical representations that do not adequately capture the complex seismic behavior of buildings and their components. To address this challenge, the new Global Vulnerability Model developed by the Global Earthquake Model (GEM) Foundation introduces a comprehensive, openly accessible database that advances seismic vulnerability modelling for structural and nonstructural components, including building contents. The database is designed to represent multiple loss types and to support both probabilistic and scenario-based seismic risk analyses. The structural component of the model includes three key advancements. First, the coverage of building classes is expanded from approximately 500 to 1,000, enabling a more detailed representation of structural systems, construction practices, and seismic code/resistance levels. Second, building response is simulated using an enhanced numerical strategy based on computationally efficient multi-degree-of-freedom stick-and-mass models. Third, analyses employ a more extensive suite of ground-motion records representative of diverse tectonic environments, including active shallow-crustal, stable continental, and subduction regions. Finally, the database provides vulnerability functions for nonstructural components and building contents, which can dominate total earthquake losses but are typically underrepresented in large-scale assessments. Nonstructural vulnerability functions are derived from region-specific storey loss models linked to peak storey drift and peak floor acceleration, while building contents losses are estimated using floor-level fragility functions coupled with a simplified binary consequence model. All models are developed consistently across the 1,000 building classes, enabling an integrated and coherent loss estimation.

Keywords: **vulnerability, structural, nonstructural, contents, regional**

1- INTRODUCTION

Earthquakes pose a major threat to life and property, with over one million deaths and nearly a trillion USD in losses recorded over the past century. These losses are largely driven by poor structural performance and the damage sustained by nonstructural components (NSCs) and building contents, which can account for more than half of building-related losses [1]. Globally, NSCs and contents represent approximately 71% of total building value, corresponding to about 290 trillion USD in GEM's 2023 Global Exposure Model. Reliable vulnerability models that address structural, non-structural, and contents losses are therefore essential for seismic risk assessments. As part of the first Global Seismic Risk Model [2], Martins and Silva [3] introduced a database of fragility and vulnerability functions covering approximately 500 building classes. Fragility functions describe the probability of exceeding pre-defined damage states conditioned on a ground-shaking intensity measure (IM), while vulnerability functions characterize the expected economic loss ratio across a range of IM levels. The building models in that database relied on single-degree-of-freedom (SDOF) oscillators assessed through nonlinear time-history analysis (NLTHA).

While that work marked an important step in making vulnerability data globally available, SDOF oscillators present significant limitations, among which is their inability to simulate storey-level demand parameters such as peak storey drift (PSD) and peak floor acceleration (PFA), which are critical for assessing damage in multi-storey buildings, particularly for NSCs and contents. They also fail to capture higher-mode

effects, inelastic demand concentrations, and complex mechanisms like soft-storey behavior. Furthermore, NSC and content losses in the original database were approximated through coarse assumptions, such as treating NSC damage as a uniform fraction of structural damage and using a single acceleration value for the entire building to estimate content losses.

To overcome these challenges, the present study introduces the new Global Vulnerability Model, which features four key innovations: (1) expansion of building classes from approximately 500 to 1,000; (2) an advanced numerical modelling strategy replacing SDOF oscillators with stick-and-mass multi-degree-of-freedom (MDOF) systems that explicitly capture storey-level demands; (3) a comprehensive ground-motion dataset covering diverse tectonic environments; and (4) new vulnerability functions for structural components, NSCs, and building contents, all derived consistently across the full range of building classes. The complete database supports GEM's 2026 Global Seismic Risk Model and is publicly available on GitHub[1].

2- METHODOLOGY

Figure 1 outlines the overall methodology adopted for the development of the new global vulnerability database. The process begins with the numerical modelling of stick-and-mass MDOF systems for approximately 1,000 building classes. Their nonlinear dynamic response is assessed via cloud-based NLTHA using an extensive suite of ground-motion records. The storey-level seismic demands (PSD and PFA) obtained from these analyses serve as the basis for deriving: (i) structural fragility and vulnerability functions based on peak storey drift thresholds and damage-to-loss ratios; (ii) non-structural vulnerability functions through region- and occupancy-specific storey loss functions (SLFs) [4] that link drift- and acceleration-sensitive component damage to storey-level demands; and (iii) building contents vulnerability functions using a floor-by-floor binary consequence model triggered by PFA exceedance of specific thresholds. Each of these steps is detailed in the following subsections. The entire numerical modelling and analysis workflow is automated through the OpenQuake Vulnerability Modeller's Toolkit (OQ-VMTK)[2], an open-source Python package that streamlines the construction of MDOF systems, execution of analyses, and derivation of fragility and vulnerability functions [5,6].

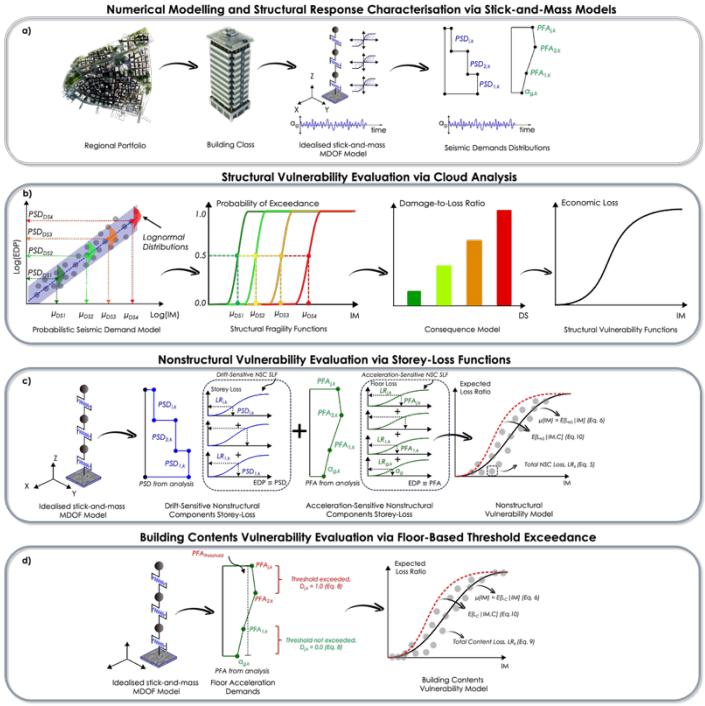


Figure 1 - Overview of the methodology for the derivation of structural, non-structural, and building contents vulnerability functions.

[1] https://github.com/gem/global_vulnerability_model
[2] https://github.com/GEMScienceTools/oq-vmtk

2-1- BUILDING CLASSES AND CAPACITY MODELS

The database expands the building classes to approximately 1,000, encompassing a broad range of vulnerability modifiers such as construction materials (reinforced concrete, steel, masonry, timber, adobe, and others), lateral load-resisting systems (moment frames, wall systems, dual systems, braced and infilled frames), seismic code levels (pre-code through high-code), ductility levels, heights, and occupancy types (residential, commercial, industrial), as illustrated in Figure 2. Each class is assigned a unique taxonomy string following GEM's building classification system (i.e., GEM Taxonomy) [7]. The nonlinear behavior of each class is described by a capacity curve in the spectral acceleration–spectral displacement domain, idealized as bilinear, trilinear, or quadrilinear shapes depending on the expected inelastic response. The capacity curves are sourced from a wide range of analytical and experimental studies and are extended to new classes by adjusting key parameters for height, ductility, and second-order effects. For more details, readers are referred to Aljawhari *et al*. [8].

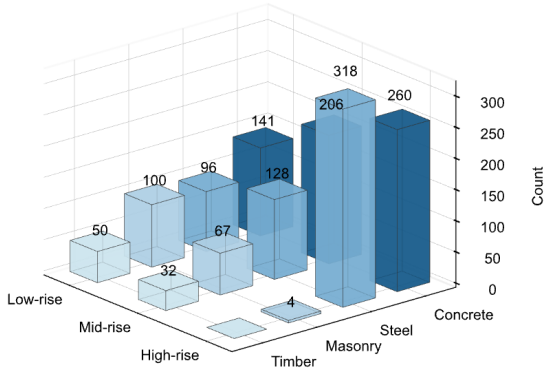


Figure 2 - Distribution of building classes according to primary vulnerability modifiers

2-2- NUMERICAL MODELLING STRATEGY

The original SDOF oscillators are replaced by stick-and-mass MDOF systems with masses lumped at each floor level and connected by nonlinear springs defining the storey shear-versus-drift behavior (Figure 1A). These models explicitly capture storey-level demands (PSD and PFA), higher-mode effects, and demand concentrations. The capacity curves are first converted to pushover curves relating roof displacement to base shear using modal participation factors. Storey-level shear force–drift relationships are then proportioned from the pushover curve based on the first-mode shape [10]. The modelling of MDOF was carried out in OpenSeesPy [9] and streamlined through the OQ-VMTK.

2-3- GROUND MOTION SELECTION AND MODIFIED CLOUD ANALYSIS

A dataset of 700 ground motion records is compiled from major international databases (e.g., NGA-W2, NGA-East, KiK-Net), spanning active shallow crustal, stable continental, and subduction tectonic regimes. Ground shaking intensity is quantified through multiple IMs tailored to building dynamics: peak ground acceleration (PGA) for low-rise structures, spectral acceleration SA at 0.3s, 0.6s, and 1.0s for low-, mid-, and high-rise classes, respectively. A small number of records are scaled (factor ≤ 2.5) to supplement the highest-intensity bins. Figure 3 illustrates the distribution of the ground motion records in terms of earthquake moment magnitude (Mw) versus Joyner–Boore distance (Rjb) and amplitude bins for the considered IM types.

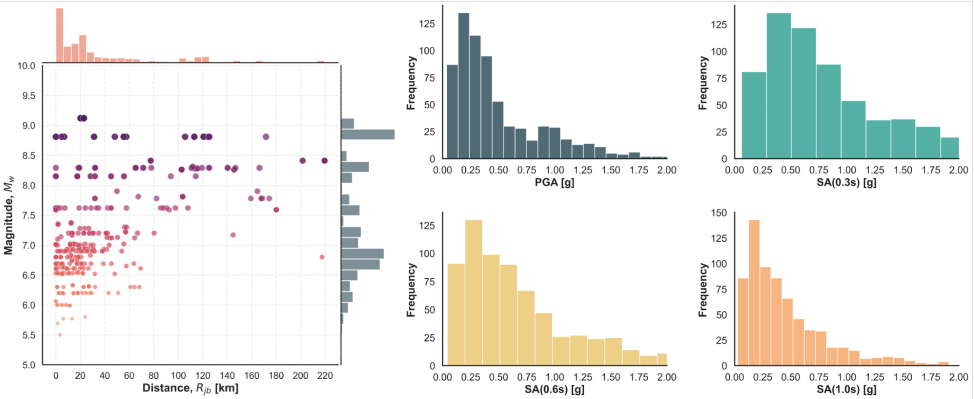


Figure 3 - Distribution of the ground motion records in terms of magnitude and distance (Mw vs. Rjb) with marginal histograms (left) of intensity measures, including PGA and spectral accelerations at 0.3 s, 1.0 s, and 3.0 s (right).

A modified cloud analysis (MCA) approach is adopted [10,11], which subjects buildings to a set of as-recorded (generally unscaled) ground motion records, thereby preserving natural correlations between intensity, frequency content, and duration, avoiding the statistical biases introduced by amplitude scaling [12,13]. The MCA extends classical cloud analysis through a dual-regression framework. First, the cloud of IM–EDP pairs is partitioned into non-collapse and collapse subsets based on a censoring threshold defined as 1.5 times the EDP at complete damage. A power-law regression is fitted in log–log space to the non-collapse observations to establish the probabilistic seismic demand model (PSDM). Simultaneously, a logistic regression model is fitted to the full dataset (with collapse treated as a binary outcome) to estimate the probability of collapse as a function of IM. The total fragility for each damage state is then computed by combining the non-collapse fragility with the collapse probability, ensuring that structural collapse is explicitly and consistently accounted for. To ensure statistical stability, particularly for building classes with few collapse observations, a bootstrapping procedure with 500 resamples is employed. In each iteration, the dataset is resampled with replacement, and both regressions are re-fitted, yielding distributions of fragility parameters from which stable mean estimates are derived. Figure 4 illustrates the modified cloud analysis procedure for a representative building class.

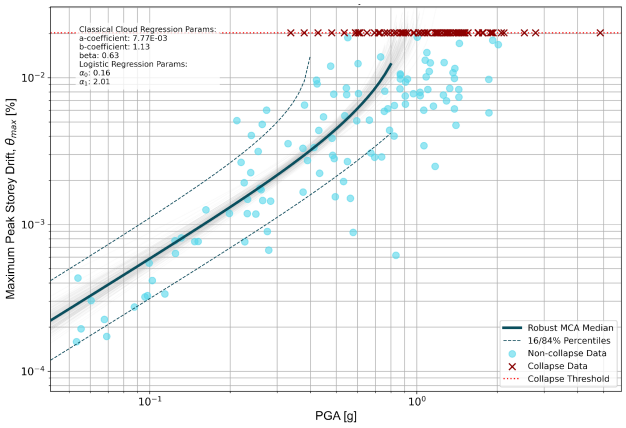


Figure 4 - Modified cloud analysis results for a representative building class

2-4- STRUCTURAL FRAGILITY AND VULNERABILITY

Structural fragility functions are derived for four damage states (DSs): slight (DS1), moderate (DS2), extensive (DS3), and complete (DS4). The onset of each DS is defined by thresholds of the maximum peak storey drift ratio, which is obtained from the stick-and-mass MDOF models and is strongly correlated with global structural damage in drift-sensitive components. The DS thresholds are adapted from the original capacity-curve-based definitions of Martins and Silva [3] and converted to the MDOF framework by transforming spectral displacement values into roof displacements, computing the corresponding interstorey drift profiles using the first-mode shape, and extracting the maximum drift across all storeys as detailed in Aljawhari *et al* [8].

Using the PSDM derived from MCA described in the previous section, fragility functions are expressed as lognormal cumulative distribution functions, as described in Equation 1:

$$[IM = im] = \Phi\left(\frac{ln\ ln\ \left(\frac{im}{\mu_i}\right)}{\beta_{TOTAL}}\right) \quad (1)$$

where Φ is the standard normal cumulative distribution function, μ_i is the median IM level at which the i-th DS is reached, and β_{TOTAL} is the total lognormal dispersion which accounts for three independent sources of uncertainty, combined via the square root of the sum of squares as per Equation 2:

$$\beta_{TOTAL} = \sqrt{\beta_{RTR}^2 + \beta_{bldg-to-bldg}^2} \quad (2)$$

where $\beta_{RTR}$is the record-to-record variability, estimated directly from the regression residuals of MCA; $\beta_{bldg-to-bldg}$is the building-to-building uncertainty, which reflects the variability arising from differences in geometric configurations, material properties, and construction quality within the same building class, and is set to a constant value of 0.3 following previous studies [3,14].

Structural vulnerability functions (Figure 1b) quantify the expected economic loss ratio over a range of IM levels, representing the repair cost of damaged structural components normalized by their replacement cost. These functions are generated by combining the DS probabilities from the fragility functions with damage-to-loss ratios (DLRs) via the total probability theorem, as per Equation (3):

$$E[IM = im] = \sum_{i=1}^{nDS} P(IM = im) * LR_{DSi} \quad (3)$$

where $P(IM = im)$ is the probability that the building is in exactly damage state DS_i at a given IM level, and LR_{DSi} is the damage-to-loss ratio associated with DS_i. The adopted mean DLR values are 0.05, 0.15, 0.60, and 1.00 for slight, moderate, extensive, and complete damage, respectively, consistent with values reported in the literature from both empirical observations and analytical procedures [15,16]. A coefficient of variation of 0.30, 0.20, 0.10, and 0.0 for slight, moderate, extensive, and complete damage, respectively, was used to represent the uncertainty in the damage-to-loss ratios [4].

The resulting discrete loss ratio observations from Equation 3 are fitted as a continuous vulnerability function using a Beta distribution [17] characterized by the mean loss ratio, E[LR|IM], and the associated coefficient of variation, CoV(IM).

2-5- NON-STRUCTURAL VULNERABILITY

Nonstructural components, such as partitions, HVAC systems, and plumbing, are vital for building functionality. Damage to these components can be caused by either PSD or PFA, which are fully represented by the new stick-and-mass MDOF models. Losses from NSC damage are quantified through SLFs, which relate storey-level losses to PSD and PFA [18]. A comprehensive dataset of region-, material-, and occupancy-specific SLFs is developed covering 12 geographic regions. NSCs are classified into drift-sensitive components (partitions, finishes, windows, stairs) and acceleration-sensitive components (HVAC, ceilings, piping, electrical systems). For each region, component inventories, fragility functions, and consequence models are compiled from the FEMA P-58 [19,20] database and regional sources. A repair cost conversion factor (RCCF) is applied to adapt North American cost data to other regions, accounting for differences in labour costs, material prices, and productivity [21–23]. SLFs are derived via Monte Carlo simulation, sampling damage states and losses for each component across a range of EDP levels. Building-level NSC vulnerability functions are obtained by combining the SLFs with storey-level PSD and PFA profiles from NLTHA, aggregating losses along the building height with appropriate weighting (Figure 1C). For the sake of brevity, readers are referred to Nafeh *et al.* [24] for more details on the derivation of SLFs and the subsequent vulnerability models associated with damage to NSCs. An example set of regional SLFs for drift- and acceleration-sensitive NSC is presented in Figure 5 for steel structures, considering different occupancy levels.

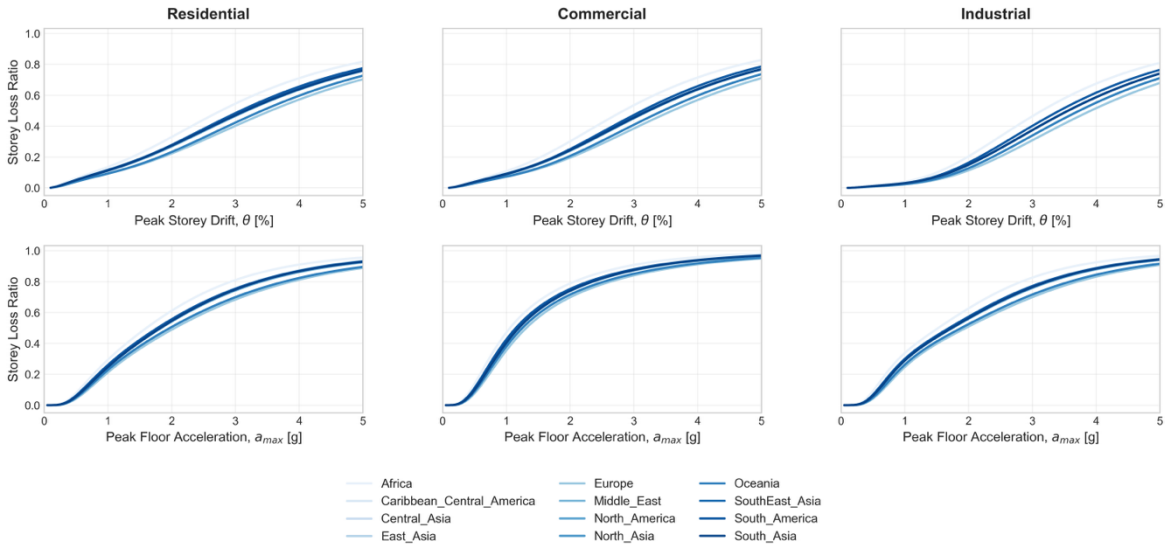


Figure 5 - Regional SLFs considering multiple occupancy types for steel structures.

2-6- BUILDING CONTENTS VULNERABILITY

Building contents encompass a broad range of items, from furniture and household electronics in residential buildings to equipment and machinery in commercial and industrial facilities. Losses associated with contents are often substantial, and their vulnerability characteristics differ from those of structural and nonstructural building components. In this study, content damage is assumed to be driven by PFA demands. To address the possibility that content damage may be focused on specific floors, content damage is modelled using a floor-by-floor binary consequence approach as illustrated in (Figure 1D): contents at each floor are classified as either undamaged or fully damaged depending on whether the local PFA exceeds an occupancy- and code-level-specific threshold derived from HAZUS guidelines (1.2g for pre- and low-code, 2.0g for moderate-code, 2.4g for high-code buildings). Floor-level losses are aggregated across the building height, assuming a uniform distribution of contents. This approach contrasts with the original database, which used a single acceleration from an SDOF model applied uniformly to the entire building.

2-7- DEPENDENCY ON STRUCTURAL DAMAGE

The vulnerability functions for NSCs and building contents are developed independently of structural damage, under the assumption that the structure remains in a repairable condition. This assumption is valid for damage states DS1 through DS3 (i.e., slight-to-extensive), where repair actions for both structural and non-structural elements are technically and economically feasible, and building contents may be partially or fully recoverable. However, when the structure reaches complete damage (DS4), which represents a state deemed irreparable (e.g., partial or total collapse), NSCs are expected to be destroyed, and building contents are generally unrecoverable. In this case, it is reasonable to assume a complete loss for both NSCs and contents, irrespective of the losses predicted by the SLFs or the binary contents model.
To incorporate this condition, the expected loss for NSCs and building contents is conditioned on the probability of complete structural damage using the total probability theorem, as per Equation 4:

$$E[IM, C] = E[IM] \times (1 - P[ds = DS_4]) + E[L, DS_4|IM] \times P[ds = DS_4|IM] \quad (4)$$

where $E[IM, C]$ is the expected loss ratio conditional on the IM and accounting for the possibility of complete structural damage; $E[IM]$ is the expected loss ratio assuming the building has not reached complete structural damage (i.e., it remains in a non-collapse, repairable state), which is derived directly from the SLFs for NSCs or from the binary consequence model for contents as described in Sections 2.5 and 2.6, respectively; $E[L, DS_4|IM]$ is the expected loss ratio at complete structural damage, which is set equal to 1.0 (i.e., total loss of NSCs or contents); and $P[ds = DS_4|IM]$ is the probability of the building reaching complete structural damage at the given IM level, extracted from the structural fragility functions.

This conditioning ensures that at low-to-moderate IM levels, where the probability of complete structural damage is negligible, the NSC and contents vulnerability functions are governed entirely by the independently derived loss models. As the IM increases and the probability of structural collapse grows, the conditioned vulnerability function progressively converges towards a total loss, reflecting the physical reality that non-structural and contents losses become irrelevant once the building has collapsed. The resulting conditioned vulnerability functions therefore provide a more realistic and internally consistent representation of total building losses across the full range of ground-shaking intensities.

Figure 6 and Figure 7 illustrate an excerpt of structural fragility and vulnerability functions derived in this study for prevalent building classes in regional building stocks, such as a two-storey non-earthquake resistant dressed stone masonry structure (MUR+STDRE/LWAL+CDN+ERN/H:2), a three-storey low-code, low earthquake resistance infilled reinforced concrete frame structure (CR/LFINF+CDL+DUL/H:3), and a seven-storey high-code, high earthquake resistance reinforced concrete structure with shear walls (CR/LWAL+CDH+ERH/H:3).

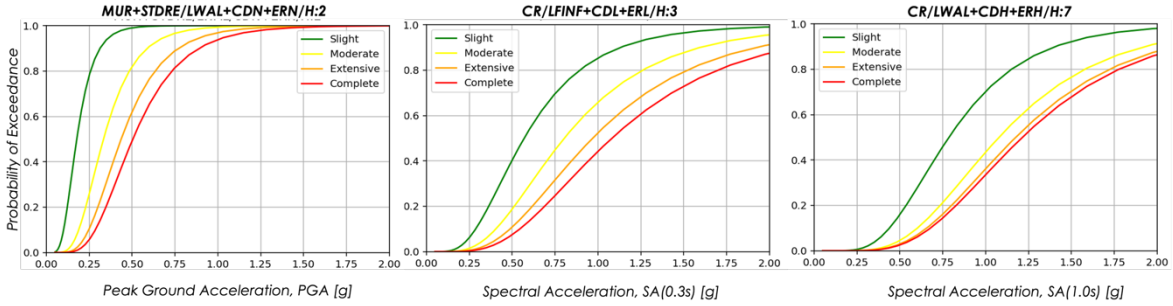


Figure 6 - Fragility functions representing the probability of exceeding a given structural damage state for the selected building classes

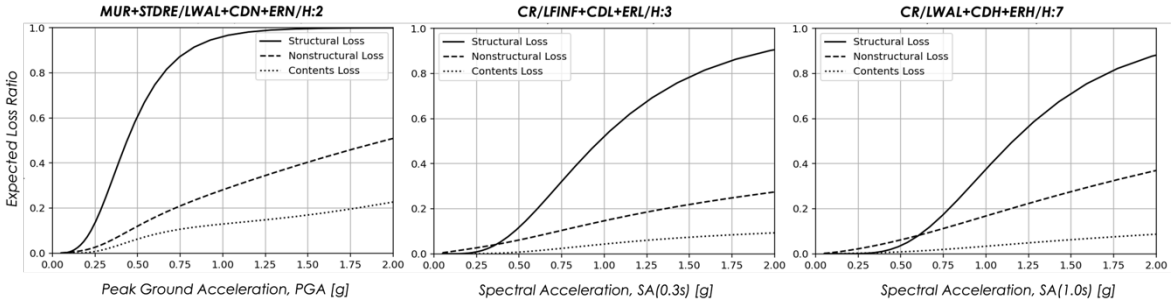


Figure 7 - Vulnerability functions for structural, nonstructural, and building contents components corresponding to a sample set of building classes from the GEM Vulnerability Database.

3- CONCLUSIONS

This study presents the most comprehensive global seismic vulnerability database to date, covering approximately 1,000 building classes and addressing structural, non-structural, and contents losses in an integrated framework. Key innovations include: (1) the transition from SDOF to stick-and-mass MDOF systems that capture storey-level demands and complex inelastic mechanisms; (2) an extensive ground-motion dataset spanning diverse tectonic environments; (3) region-, material-, and occupancy-specific storey loss functions for NSCs, derived from detailed component inventories, fragility and consequence models across 12 global regions; and (4) a floor-by-floor binary consequence approach for building contents using local PFA demands. The entire framework is implemented in the open-source OpenQuake Vulnerability Modeller's Toolkit (OQ-VMTK), and all models, data, and tools are publicly available. Additionally, a comprehensive documentation of the model inputs, outputs and underlying assumption is hosted on a dedicated website[3].

[3] https://docs.openquake.org/vulnerability/

2. REFERENCES

[1] Yepes-Estrada C, Calderon A, Costa C, Crowley H, Dabbeek J, Hoyos MC, et al. Global building exposure model for earthquake risk assessment. Earthquake Spectra 2023;39:2212–35. https://doi.org/10.1177/87552930231194048.

[2] Silva V, Amo-Oduro D, Calderon A, Costa C, Dabbeek J, Despotaki V, et al. Development of a global seismic risk model. Earthquake Spectra 2020;36:372–94. https://doi.org/10.1177/8755293019899953.

[3] Martins L, Silva V. Development of a fragility and vulnerability model for global seismic risk analyses. Bulletin of Earthquake Engineering 2021;19:6719–45. https://doi.org/10.1007/s10518-020-00885-1.

[4] Ramirez C, Miranda E. Building-specific loss estimation methods and tools for simplified performance-based earthquake engineering. Stanford: 2009.

[5] Nafeh AMB, Aljawhari K, Silva V, Ettorre A, Crowley H. OQ-VMTK: An Open-Source Toolkit for Earthquake Vulnerability Modelling Applications. Earthquake Spectra (In Press) 2026.

[6] Nafeh AMB, Aljawhari K, Ettorre A, Silva V, Crowley H. OpenQuake Vulnerability Modeller's Toolkit (VMTK) v1.0.0 2025.

[7] Silva V, Brzev S, Scawthorn C, Yepes C, Dabbeek J, Crowley H. A Building Classification System for Multi-hazard Risk Assessment. International Journal of Disaster Risk Science 2022;13:161–77. https://doi.org/10.1007/s13753-022-00400-x.

[8] Aljawhari K, Nafeh AMB, Silva V. An Improved Global Vulnerability Model for Seismic Risk Assessment: Part 1 – Structural Vulnerability. Bulletin of Earthquake Engineering (In Press) 2026. https://doi.org/https://doi.org/10.21203/rs.3.rs-7935593/v1.

[9] Zhu M, McKenna F, Scott MH. OpenSeesPy: Python library for the OpenSees finite element framework. SoftwareX 2018;7:6–11. https://doi.org/10.1016/j.softx.2017.10.009.

[10] Jalayer F, De Risi R, Manfredi G. Bayesian Cloud Analysis: efficient structural fragility assessment using linear regression. Bulletin of Earthquake Engineering 2015;13:1183–203. https://doi.org/10.1007/s10518-014-9692-z.

[11] Jalayer F, Ebrahimian H, Miano A, Manfredi G, Sezen H. Analytical fragility assessment using unscaled ground motion records. Earthq Eng Struct Dyn 2017;46:2639–63. https://doi.org/10.1002/eqe.2922.

[12] Dávalos H, Miranda E. Evaluation of bias on the probability of collapse from amplitude scaling using spectral-shape-matched records. Earthq Eng Struct Dyn 2019;48:970–86. https://doi.org/10.1002/eqe.3172.

[13] Nafeh AMB, O'Reilly GJ. Unbiased simplified seismic fragility estimation of non-ductile infilled RC structures. Soil Dynamics and Earthquake Engineering 2022;157:107253. https://doi.org/10.1016/j.soildyn.2022.107253.

[14] ATC. Quantification of building seismic performance factors. 2009.

[15] Aljawhari K, Gentile R, Galasso C. Simulation-based consequence models of seismic direct loss and repair time for archetype reinforced concrete frames. Soil Dynamics and Earthquake Engineering 2023;172:107979. https://doi.org/10.1016/j.soildyn.2023.107979.

[16] Del Vecchio C, Ludovico M Di, Prota A. Repair costs of reinforced concrete building components: from actual data analysis to calibrated consequence functions. Earthquake Spectra 2020;36:353–77. https://doi.org/10.1177/8755293019878194.

[17] Shome N, Jayaram N, Rahnama M. Uncertainty and spatial correlation models for earthquake losses. 15th World Conference on Earthquake Engineering. Lisbon, Portugal, 2012.

[18] Nafeh A, O'Reilly GJ. Simplified pushover-based seismic loss assessment for existing infilled frame structures. Bulletin of Earthquake Engineering 2024;22:951–95. https://doi.org/10.1007/s10518-023-01792-x.

[19] Federal Emergency Management Agency (FEMA). FEMA P-58-1, Seismic Performance Assessment of Buildings, Volume 1 – Methodology. Washington, DC.: 2018.

[20] Federal Emergency Management Agency (FEMA). FEMA P-58-2, Seismic Performance Assessment of Buildings, Volume 2 – Implementation Guide. Washington, DC: 2018.

[21] Silva A, Castro JM, Monteiro R. A rational approach to the conversion of FEMA P-58 seismic repair costs to Europe. Earthquake Spectra 2020;36:1607–18. https://doi.org/10.1177/8755293019899964.

[22] Papadopoulos AN, Roth P, Danciu L, Bergamo P, Panzera F, Fäh D, et al. The Earthquake Risk Model of Switzerland, ERM-CH23. Natural Hazards and Earth System Sciences 2024;24:3561–78. https://doi.org/10.5194/nhess-24-3561-2024.

[23] Porter K, Farokhnia K, Vamvatsikos D, Cho I. Guidelines for component-based analytical vulnerability assessment of buildings and nonstructural elements. Pavia: 2015.

[24] Nafeh AMB, Aljawhari K, Silva V. An Improved Global Vulnerability Model for Seismic Risk Assessment: Part 2 – Non-Structural and Contents Vulnerability. Bulletin of Earthquake Engineering (In Press) 2026.